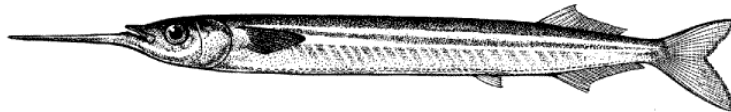


**EARLY LIFE STAGES OF THE SOUTHERN SEA GARFISH,  
*HYPORHAMPHUS MELANOCHIR* (VALENCIENNES, 1846),  
AND THEIR ASSOCIATION WITH SEAGRASS BEDS**

**CRAIG J. NOELL**



SCHOOL OF EARTH AND ENVIRONMENTAL SCIENCES  
THE UNIVERSITY OF ADELAIDE  
SOUTH AUSTRALIA

*Submitted for the Degree of Doctor of Philosophy  
on January 11, 2005*

## TABLE OF CONTENTS

<b>List of tables</b>	<b>v</b>
<b>List of figures</b>	<b>vii</b>
<b>Abstract</b>	<b>xi</b>
<b>Declaration</b>	<b>xiii</b>
<b>Acknowledgments</b>	<b>xiv</b>
<b>CHAPTER 1 GENERAL INTRODUCTION</b>	<b>1</b>
1.1 BACKGROUND	1
1.2 LITERATURE REVIEW	2
1.2.1 Distribution and taxonomy	2
1.2.2 Reproduction and early life history	3
1.2.3 Age and growth	4
1.2.4 Diet	4
1.3 SIGNIFICANCE OF SEAGRASS TO <i>H. MELANOCHIR</i>	6
1.4 OVERALL AIMS AND STRUCTURE OF THESIS	7
1.5 OBJECTIVES	8
<b>CHAPTER 2 REPRODUCTIVE BIOLOGY</b>	<b>9</b>
2.1 INTRODUCTION	9
2.2 MATERIALS AND METHODS	10
2.2.1 Collection of fish	10
2.2.2 Laboratory procedures	10
2.2.2.1 <i>Processing of fish</i>	10
2.2.2.2 <i>Histological preparation</i>	12
2.2.2.3 <i>Transmission electron microscopy</i>	12
2.2.3 Statistical analyses	13
2.3 RESULTS	14
2.3.1 Stages of oocyte development	14
2.3.1.1 <i>Perinucleolar stage</i>	14
2.3.1.2 <i>Yolk vesicle formation</i>	14
2.3.1.3 <i>Yolk globule stage</i>	14
2.3.1.4 <i>Migratory nucleus stage</i>	16
2.3.1.5 <i>Hydrated stage</i>	16
2.3.2 Oocyte filaments	16
2.3.3 Proportion and size distribution of oocytes	16
2.3.4 Sexual maturity and fecundity	19
2.3.5 Female-male characteristics	20
2.3.6 Reproductive seasonality	21
2.4 DISCUSSION	23

<b>CHAPTER 3 MOLECULAR DISCRIMINATION OF <i>HYPORHAMPHUS</i> LARVAE</b>	<b>30</b>
3.1 INTRODUCTION	30
3.2 MATERIALS AND METHODS	31
3.2.1 Specimens examined	31
3.2.2 DNA extraction, PCR amplification, and nucleotide sequencing	33
3.2.3 Phylogenetic analysis	33
3.2.4 PCR test for species identification	34
3.3 RESULTS	34
3.4 DISCUSSION	36
<b>CHAPTER 4 LARVAL DEVELOPMENT OF <i>H. MELANOCHIR</i> AND <i>H. REGULARIS</i></b>	<b>39</b>
4.1 INTRODUCTION	39
4.2 MATERIAL AND METHODS	40
4.3 RESULTS	43
4.3.1 <i>Hyporhamphus melanochir</i>	43
4.3.1.1. <i>Description of larvae</i>	43
4.3.1.2. <i>Development of fins</i>	43
4.3.1.3. <i>Pigmentation</i>	44
4.3.2 <i>Hyporhamphus regularis</i>	46
4.3.2.1. <i>Description of larvae</i>	46
4.3.2.2. <i>Development of fins</i>	48
4.3.2.3. <i>Pigmentation</i>	48
4.3.3 Logistic regression analysis of body measurements	48
4.4 DISCUSSION	52
<b>CHAPTER 5 DISTRIBUTION, AGE, GROWTH AND BACK-CALCULATED SPAWNING DATES OF LARVAE</b>	<b>55</b>
5.1 INTRODUCTION	55
5.2 MATERIALS AND METHODS	58
5.2.1 Collection of eggs	58
5.2.2 Collection of larvae	60
5.2.3 Distribution and abundance of larvae	61
5.2.4 Effectiveness of method for collection of larvae	61
5.2.5 Spatial analysis of larval abundances	62
5.2.6 Age and growth of larvae	63
5.2.7 Back-calculation of hatching and spawning dates	64
5.2.8 Wind data	65
5.3 RESULTS	65
5.3.1 Collection of <i>H. melanochir</i> eggs	65
5.3.2 Distribution and abundance of larvae	66
5.3.3 Spatial analysis of larval abundances	70

5.3.4 Age and growth of larvae and back-calculated spawning dates	70
5.3.5 Wind data	71
5.4 DISCUSSION	72
<b>CHAPTER 6 ASSIMILATION OF SEAGRASS IN THE DIET</b>	<b>79</b>
6.1 INTRODUCTION	79
6.2 MATERIALS AND METHODS	81
6.2.1 Study area	81
6.2.2 Collection of <i>H. melanochir</i> , potential food sources and other fish	81
6.2.3 Processing and stable isotope analysis	83
6.2.4 Trophic levels	84
6.2.5 Standard linear mixing models	84
6.2.6 Uncertainty in source proportion estimates	85
6.2.7 Concentration-weighted mixing model	86
6.3 RESULTS	86
6.3.1 Carbon isotope values	86
6.3.2 Nitrogen isotope values and trophic levels	86
6.3.3 Relative contributions of food sources to the diet of <i>H. melanochir</i>	87
6.3.3.1. <i>Two-source linear mixing model</i>	87
6.3.3.2. <i>Three-source linear mixing model</i>	90
6.3.3.3. <i>Concentration-dependent mixing model</i>	90
6.4 DISCUSSION	90
<b>CHAPTER 7 GENERAL DISCUSSION</b>	<b>98</b>
7.1 OVERVIEW	98
7.2 EXPERIMENTAL FINDINGS	98
7.2.1 Reproductive biology	98
7.2.2 Early life stages	100
7.2.3 Distribution of larvae	101
7.2.4 Diet	103
7.3 DIRECTIONS FOR FURTHER RESEARCH	104
7.4 IMPLICATIONS TOWARDS MANAGEMENT	104
<b>Appendices</b>	<b>107</b>
<b>References</b>	<b>126</b>

## List of tables

TABLE 2.1 Descriptions of the eight macroscopic stages of development of the ovaries of <i>Hyporhamphus melanochir</i> (modified with permission from Ling, 1958).	11
TABLE 2.2 Brief descriptions of stages of oocyte development in teleosts (from West, 1990).	13
TABLE 2.3 Monthly sex ratios of <i>Hyporhamphus melanochir</i> and results of chi-square ( $\chi^2$ ) goodness of fit tests.	21
TABLE 2.4 Classification and description of whole oocytes within ripe ovaries of <i>Hyporhamphus melanochir</i> (reproduced with permission from Ling, 1958).	24
TABLE 3.1 Sample details of garfish examined for mitochondrial DNA variation. $n_s$ indicates sample size for nucleotide sequencing; $n_{PCR}$ indicates sample size for PCR assay. Locality codes are in parentheses.	31
TABLE 3.2 Oligonucleotide sequences of primers used to discriminate garfish <i>Hyporhamphus</i> species found in southern Australian waters.	33
TABLE 4.1 Morphometrics of larval, transforming larval, and juvenile <i>Hyporhamphus melanochir</i> (expressed as a percentage of $L_B$ ). Mean $\pm$ 1 S.D. is given when sample size $n > 1$ . Dotted lines differentiate larvae, transforming larvae, and juveniles in descending order.	45
TABLE 4.2 Meristic counts of larval, transforming larval, and juvenile <i>Hyporhamphus melanochir</i> . Numbers in bold indicate the $L_B$ at which a full complement of rays is first attained. Dotted lines differentiate larvae, transforming larvae, and juveniles in descending order. D, dorsal; A, anal; P <sub>1</sub> , pectoral; P <sub>2</sub> , pelvic; C, caudal.	46
TABLE 4.3 Morphometrics of larval, transforming larval, and juvenile <i>Hyporhamphus regularis</i> (expressed as a percentage of $L_B$ ). Mean $\pm$ 1 S.D. is given when sample size $n > 1$ . Dotted lines differentiate larvae, transforming larva, and juveniles in descending order.	49
TABLE 4.4 Meristic counts of larval, transforming larval, and juvenile <i>Hyporhamphus regularis</i> . Numbers in bold indicate the $L_B$ at which a full complement of rays is first attained. Dotted lines differentiate larvae, transforming larva, and juveniles in descending order. D, dorsal; A, anal; P <sub>1</sub> , pectoral; P <sub>2</sub> , pelvic; C, caudal.	50
TABLE 4.5 Summary of statistics for independent variables included in the logistic regression model used to distinguish between <i>Hyporhamphus melanochir</i> and <i>H. regularis</i> larvae. Regression coefficient ( $B$ ) is given as maximum likelihood estimate $\pm$ 1 S.E.	51
TABLE 4.6 Classification matrix for the logistic regression model used to distinguish between <i>Hyporhamphus melanochir</i> and <i>H. regularis</i> larvae. For each cell, the number on the left denotes the analysis sample and the number on the right denotes the holdout sample. Hit ratio is the percentage correctly classified.	51
TABLE 4.7 Meristic counts of adult hemiramphids found in southern Australia. Data collated from Collette (1974) except where footnoted. A second range from another source is given if not in total agreement with Collette (1974). The distinguishing vertebral counts for <i>H. melanochir</i> and <i>H. regularis</i> in this study are also included. Vertebrae are given as precaudal + caudal; gill rakers are given as upper + lower. ? = no information available. D, dorsal; A, anal; P <sub>1</sub> , pectoral; P <sub>2</sub> , pelvic; C, caudal.	54
TABLE 5.1 Review of the literature on Beloniform eggs that have filaments used for attachment to fixed or floating objects. ? Information not available.	56
TABLE 5.2 Summary of two-factor ANOVA with replication to test for significance of type of sampling gear and time of day on abundance of <i>Hyporhamphus melanochir</i> larvae.	69
TABLE 5.3 Estimates of Laird-Gompertz growth function parameters for <i>Hyporhamphus melanochir</i> larvae collected from gulf waters of South Australia.	71
TABLE 5.4 Growth rate (mm d <sup>-1</sup> and % d <sup>-1</sup> ) of <i>Hyporhamphus melanochir</i> larvae from gulf waters of South Australia estimated from the Laird-Gompertz growth function.	72

- TABLE 6.1 Stable isotope data used in standard mixing model and concentration-dependent model calculations (except data for fish species above the dotted line, which are for comparison only). Values for stable carbon- and nitrogen-isotope ratios are given as mean  $\pm$  1 S.D. The numbers in parentheses refer to the ranges of standard length ( $L_s$ , mm). 82
- TABLE 6.2 Relative contributions ( $f$ , in %) of food sources (X and Y) in the diets of larval, juvenile and adult *Hyporhamphus melanochir* estimated by the two-source mixing model. Values for  $f$  are given as **mean**  $\pm$  1 S.E. The 95% confidence interval (C.I.) was not calculated for larval food sources since only one pooled sample of larvae was analysed. Combinations are only given where  $0 \leq f \leq 100\%$  for all sources; these are listed in alphanumeric order. Boxes indicate the combinations where *Zostera* is the main plant food source. 89
- TABLE 6.3 Relative contributions ( $f$ , in %) of food sources (X, Y, and Z) in the diets of larval and juvenile *Hyporhamphus melanochir* estimated by the three-source mixing model. Values for  $f$  are given as **mean**  $\pm$  1 S.E. The 95% confidence interval (C.I.) was not calculated for larval food sources since only one pooled sample of larvae was analysed. Combinations are only given where  $0 \leq f \leq 100\%$  for all sources; these are listed in alphanumeric order. Boxes indicate the combinations where *Zostera* is the main plant food source. 91
- TABLE 6.4 Relative contributions ( $f$ , in %) of three food sources (X, Y, and Z) in the diet of juvenile *Hyporhamphus melanochir* estimated by the concentration-dependent model. As defined by Phillips & Koch (2002),  $f_{X,B}$ ,  $f_{Y,B}$ , and  $f_{Z,B}$  represent the fractions of assimilated biomass of sources in the mixture (equivalent to  $f_X$ ,  $f_Y$ , and  $f_Z$  in the standard mixing model, indicated in boldface). Similarly,  $f_{X,C}$ ,  $f_{Y,C}$ ,  $f_{Z,C}$ ,  $f_{X,N}$ ,  $f_{Y,N}$ , and  $f_{Z,N}$  represent the fractions of assimilated C or N of the individual sources in the mixture. Combinations are only given where  $0 \leq f \leq 100\%$  for all sources after rounding; these are listed in alphanumeric order. 92
- TABLE 6.5 Taxonomy of zooplankton positively identified among the gut contents of *Hyporhamphus melanochir* larvae. These food items were incidentally found after larvae were cleared and stained for the examination of fin and vertebrae meristics (Chapter 4). Taxa are listed in alphabetical order. 95

## List of figures

- FIG. 2.1 Histological features of ovarian and oocyte development for *Hyporhamphus melanochir* stained with haematoxylin and eosin. (a) Partial cross section of a stage III ovary showing the presence of all oocyte stages except hydrated; (b) Early perinucleolar; (c) late perinucleolar; (d) early yolk vesicle; (e) yolk vesicle; (f) yolk globule; (g) migratory nucleus; (h) late migratory nucleus; (i) hydrated; (j) enlargement of detail of hydrated. Abbreviations: *P* perinucleolar; *YV* yolk vesicle; *YG* yolk globule; *MN* migratory nucleus; *c* cytoplasm; *f* filaments; *n* nucleus; *no* nucleoli; *yg* yolk globules; *ym* yolk mass; *yv* yolk vesicles; *zr* zona radiata. Scale bars: (a), (i) 500  $\mu\text{m}$ ; (b), (c) 50  $\mu\text{m}$ ; (d), (j) 100  $\mu\text{m}$ ; (e), (f), (g), (h) 200  $\mu\text{m}$ . 15
- FIG. 2.2 Partial cross section of an oocyte filament (*f*) from a hydrated oocyte of *Hyporhamphus melanochir* stained with ruthenium red showing the adhesive layer of mucopolysaccharides (*m*). A line drawing of an ovulated oocyte and filament is included to orientate the image. 17
- FIG. 2.3 Hydrated oocytes (two ovulated, five unovulated) teased out from a running ripe ovary of *Hyporhamphus melanochir*. Note: the remnant material from deterioration of the follicular layer, i.e. postovulatory follicle, indicated by arrows. 17
- FIG. 2.4 Percentage frequencies of oocyte developmental stages (mean + 1 S.D.) in ovaries of *Hyporhamphus melanochir*. Abbreviations for oocyte stages: *P* perinucleolar; *YV* yolk vesicle; *YG* yolk globule; *MN* migratory nucleus; *H* hydrated. Numbers of oocytes and ovaries (in parentheses) are given for each ovarian stage. 18
- FIG. 2.5 Percentage frequency distributions of oocyte diameters (shaded area) and proportional volume (unshaded area) in ovaries of *Hyporhamphus melanochir*. Ovarian stages: (a) II; (b) III; (c) IV; (d) V; (e) VI; (f) VII. Abbreviations for oocyte stages as for FIG. 2.4. Number of oocytes is given for each ovarian stage. Data are presented for 50- $\mu\text{m}$  size classes and smoothed with a moving average of three. 19
- FIG. 2.6 Proportions of ovarian stages by standard length ( $L_S$ ) class of *Hyporhamphus melanochir*. Also shown is the logistic curve that estimates the probability that females are mature at a given  $L_S$ . The vertical drop line indicates  $L_{50}$ . Number of fish is given for each  $L_S$  class. 20
- FIG. 2.7 Relationships between (a) batch fecundity ( $F_B$ ) and standard length ( $L_S$ ) and (b)  $\log_{10}F_B$  and ovary-free fish weight ( $W_F$ ) of *Hyporhamphus melanochir*. See text for regression and correlation results. 20
- FIG. 2.8 Gonadosomatic indices ( $I_G$ , mean  $\pm$  1 S.E.) for female and male *Hyporhamphus melanochir* from October 1998 to May 2000. To improve clarity of presentation, data for the December 2001 sample was excluded. The spline curve represents the moving average of female  $I_G$  with a sampling proportion of 0.2. 22
- FIG. 2.9 Monthly percentage compositions of ovarian stages of *Hyporhamphus melanochir*. Data were pooled for a calendar year. Number of fish is given for each month. 22
- FIG. 2.10 Monthly distributions of average maximum oocyte diameters of *Hyporhamphus melanochir*. Boxes enclose values between the 25<sup>th</sup> and 75<sup>th</sup> percentiles; whiskers are the 10<sup>th</sup> and 90<sup>th</sup> percentiles; thin and thick horizontal lines are median and mean values, respectively; and each data point is an outlier representing one fish. Data were pooled for a calendar year. Number of fish is given for each month. 23
- FIG. 3.1 Map of southern Australia showing the locations from which garfish were sampled for the examination of mitochondrial DNA variation. Details of sample sizes and life stages are given in TABLE 3.1. 32
- FIG. 3.2 Phylogenetic relationships among garfish *control region* haplotypes recovered with maximum parsimony. Unbolded numerals represent bootstrap proportions from 2000 pseudoreplicates; numerals in boldface are the number of sites that change along that branch. Refer to TABLE 3.1 for locality codes. 35

- FIG. 3.3 A section (nucleotide sites 155 to 210) of the complete sequence alignment (APPENDIX B) of mitochondrial *control region* haplotypes from adult and larval *Hyporhamphus melanochir* and *H. regularis*, *H. australis*, and the outgroup *Arrhamphus sclerolepis*. The oligonucleotide sequence of the PCR primer L-M282 (boxed), used to discriminate between *H. melanochir* and *H. regularis*, was designed from this section of the alignment; introduced mismatches in the sequence are given in lowercase. Dots (.) indicate identical nucleotides to *H. melanochir* larva; dashes (-) indicate alignment gaps; question mark (?) indicates unknown nucleotide. Refer to TABLE 3.1 for locality codes. 36
- FIG. 3.4 Electrophoretic discrimination between mtDNA *control region* multiplex PCR products from *Hyporhamphus melanochir* (443 bp) and *H. regularis* (462 and 264 bp). Lanes 1 and 2, *H. melanochir* larvae; lanes 3 and 4, *H. regularis* larvae; lane 5, *H. melanochir* adult; lane 6, *H. regularis* adult; lane 7, no template PCR control. M indicates 100-bp ladder for molecular weight marker. The positions of the respective DNA products are indicated by arrows. 37
- FIG. 4.1 Body measurements used to describe larval *Hyporhamphus melanochir* and *H. regularis*. Abbreviations:  $B_A$ , body depth at anus;  $B_P$ , body depth at pectoral base;  $D_{EH}$ , horizontal eye diameter;  $D_{EV}$ , vertical eye diameter;  $L_B$ , body length;  $L_H$ , head length;  $L_{LJ}$ , lower jaw length;  $L_{LJx}$ , lower jaw extension;  $L_{PA}$ , preanal length;  $L_{PD}$ , pre dorsal-fin length;  $L_{Sn}$ , snout length. Drawing of larva reproduced with permission from Bruce (1989). 41
- FIG. 4.2 Cleared and stained *Hyporhamphus melanochir* (a) larva (11.0 mm) and (b) juvenile (33.3 mm) for the purpose of counting fin rays and vertebrae. 41
- FIG. 4.3 Larval, transforming larval, and juvenile *Hyporhamphus melanochir*. (a) 6.4 mm reared yolk-sac larva; newly hatched (redrawn from Jordan *et al.*, 1998) (L 3072-01); (b) 9.3 mm larva (L 3073-01); (c) 13.3 mm larva (composite drawing of two damaged larvae of same  $L_B$ ) (L 3073-02 and -03); (d) 20.4 mm transforming larva (L 3074-01), myomeres omitted; (e) 29.3 mm juvenile (L 3074-02), myomeres omitted. 44
- FIG. 4.4 Pigmentation of an 8.5 mm *Hyporhamphus melanochir* larva. (a) Dorsal view, arrows indicate the margins of the 12-15 melanophore pairs in longitudinal rows; (b) ventral view. 47
- FIG. 4.5 Larval and juvenile *Hyporhamphus regularis*. (a) 7.1 mm yolk-sac larva (L 3076-01); (b) 9.4 mm larva (L 3076-02); (c) 12.3 mm larva (L 3076-03); (d) 15.5 mm larva (L 3076-04), myomeres omitted; (e) 24.7 mm juvenile (L 3077-01). 47
- FIG. 4.6 Pigmentation of a 8.7 mm *Hyporhamphus regularis* larva. (a) Dorsal view, arrows indicate the margins of the 19-22 melanophore pairs in longitudinal rows; (b) Ventral view, arrow indicates the ventral pigment blotch. 50
- FIG. 4.7 Relationship between the unadjusted horizontal eye diameter to body length ratio ( $D_{EH}/L_B$ , in percentage) and  $L_B$  (mm) for *Hyporhamphus melanochir* and *H. regularis* larvae and juveniles. 51
- FIG. 4.8 Adjusted horizontal eye diameter ( $D_{EH}$ ) and pre-dorsal fin length ( $L_{PD}$ ) of *Hyporhamphus melanochir* and *H. regularis* larvae. Data represent analysis and holdout samples and are superimposed on a 3D-mesh plot of the logistic regression model used to distinguish between *Hyporhamphus melanochir* and *H. regularis* larvae. The line bisecting the mesh plot indicates the 0.5 probability cutoff score for predicting species. 52
- FIG. 5.1 Map of Gulf St Vincent showing land-based wind measurement stations (◆) and the locations that were searched for *Hyporhamphus melanochir* eggs (●). 59
- FIG. 5.2 (a) Side and (b) front views of the beam trawl used to sample benthic habitat for the collection of *Hyporhamphus melanochir* eggs. Note: the digital video camera mounted on top of the trawl frame. 60
- FIG. 5.3 (a) Hauling and (b) operation of the neuston net used to collect *Hyporhamphus melanochir* larvae. 61
- FIG. 5.4 Photomicrographs of lapilli from *Hyporhamphus melanochir* larvae, estimated to be (a) 9 and (b) 12 days of age after the presumed hatch mark (\*). Each dot corresponds to the discontinuous zone of a daily growth increment (one daily growth increment = discontinuous zone + accretion zone). Both photomicrographs are at the same scale. 64



- FIG. 5.5 A *Hyporhamphus melanochir* egg attached to the algal epiphyte *Jania* on seagrass *Posidonia*. 66
- FIG. 5.6 Abundance of *Hyporhamphus melanochir* larvae in the Bay of Shoals during Mar 3-5, 2000, collected with a neuston net and subsurface net during day and night. (a) neuston at day; (b) neuston at night; (c) subsurface at day; (d) subsurface at night. Densities of larvae are the same as for the legend in (a). Also shown are the densities of seagrass habitat: ■ sparse; ■ medium; ■ dense; ■ patchy (from Edyvane, 1999). 67
- FIG. 5.7 Distribution and abundance of *Hyporhamphus melanochir* larvae in Gulf St Vincent during (a) Dec 14-17, 1998 (cruise 1) and (b) Dec 4-7, 2000 (cruise 3) aboard RV *Ngerin*. Also shown are the densities of seagrass habitat: ■ sparse; ■ medium; ■ dense; ■ patchy (from Edyvane, 1999). 68
- FIG. 5.8 Length-frequency distribution of *Hyporhamphus melanochir* larvae from Gulf St Vincent collected on (a) Dec 14-17, 1998 (cruise 1, n = 108) and (b) Dec 4-7, 2000 (cruise 3, n = 310). Note: some larvae from cruise 3 could not be measured due to damage or poor preservation. 69
- FIG. 5.9 Correlogram of Moran's *I* statistic v. distance class for abundances of *Hyporhamphus melanochir* larvae in Gulf St Vincent on Dec 14-17, 1998 (cruise 1) and Dec 4-7, 2000 (cruise 3). The width of each distance class is 10.65 km. Autocorrelation values significant at  $\alpha = 0.05$  are indicated with solid circles. Histogram shows the number of neighbour pairs at each distance class (2<sup>nd</sup> Y-axis). 70
- FIG. 5.10 Estimated age ( $\pm 1$  S.E.) v. body length for *Hyporhamphus melanochir* larvae from Gulf St Vincent and Spencer Gulf, South Australia. The curve was fitted using the Laird-Gompertz growth function. Parameters of the model are shown in TABLE 5.3. 71
- FIG. 5.11 Spawning date distributions for *H. melanochir* larvae collected from Gulf St Vincent during Dec 14-17, 1998 (cruise 1) and Dec 4-7, 2000 (cruise 3), and from Spencer Gulf and Gulf St Vincent during Jan 31-Feb 5, 1999 (cruise 2). Spawning dates were back-calculated by subtracting the estimated age and the predicted egg incubation period from the date of capture. Data are presented in the same calendar year. Horizontal bars indicate the duration of cruises during which samples were collected. 72
- FIG. 5.12 Incident wind vectors ( $m\ s^{-1}$ , degrees True) recorded at three-hourly intervals from seven land-based wind measurement stations situated around Gulf St Vincent during (a) Oct 1-Dec 17, 1998 and (b) Oct 1-Dec 7, 2000. 73
- FIG. 5.13 Percentages of winds (directions and speeds) recorded at three-hourly intervals from seven land-based wind measurement stations situated around Gulf St Vincent for (a) Oct 1-Dec 17, 1998 ( $n = 3723$  readings) and (b) Oct 1-Dec 7, 2000 ( $n = 3650$  readings). Calms included at centre of wind rose. Rings are at 5% intervals. Wind flow is *from* the directions shown. 74
- FIG. 6.1 Bivariate plot of the stable carbon- and nitrogen-isotope ratios (mean  $\pm 1$  S.D.) of fish (blue text, except *Hyporhamphus melanochir*, which is black), seagrass (green), algae (brown) and plankton (red) in the Bay of Shoals. \*Larval *H. melanochir*; †juvenile *H. melanochir*; ‡adult *H. melanochir*. Classification of trophic level was based on a 3.4‰ increase in  $\delta^{15}N$  from one level to the next. 87
- FIG. 6.2 Examples for estimating proportions (in parentheses) of different food sources in the diet of juvenile *Hyporhamphus melanochir* using (a) two- and (b) three-source standard mixing models and (c) the concentration-dependent model. Stable isotope ratios are shown for *H. melanochir* and food sources. The prime symbol (') indicates values are corrected for fractionation. Error bars show  $\pm 1$  S.E. (inner bars) and 95% C.I. (outer bars). Note: in the bivariate plots of the two isotopes, the mean composition of the consumer falls within the mixing triangle in (b) but not in (c). The vertices of each triangle represent the position of the consumer if its diet consisted exclusively of a particular food source. Lines within the triangle are 'iso-diet' lines, along which the proportion of a food source is invariant. Iso-diet lines are shown at 25% intervals, from 100% at the vertex to 0% along the side of the triangle opposite the vertex. 88

FIG. 6.3 Photomicrographs of zooplankton found in the gut contents of *Hyporhamphus melanochir* larvae after the larvae were cleared and stained for fin and vertebrae meristics. Both photomicrographs are at the same scale.

95

## Abstract

This study investigates early life stages of the southern sea garfish (*Hyporhamphus melanochir*) and their association with seagrass in Gulf St Vincent, South Australia. The overall aims were to identify and describe the early life stages of *H. melanochir* and to explore the possible relationship(s) between these life stages and seagrass habitat with the emphasis on seagrass as a requirement for spawning or as a food source.

The reproductive biology of female *H. melanochir* from the commercial fishery was assessed by microscopic examination of ovaries, oocyte size distributions, gonadosomatic indices, and macroscopic ovarian stages. Five stages of oocyte development were identified and described: perinucleolar, yolk vesicle, yolk globule, migratory nucleus and hydrated. A coherence between histological and whole oocyte descriptions is demonstrated. *Hyporhamphus melanochir* are characterised as multiple spawners with group-synchronous oocyte development and indeterminate fecundity. A protracted spawning season from October to March was indicated by the occurrence of ripe ovaries and increases in gonadosomatic index. Females reach sexual maturity at 193 mm standard length, and batch fecundity ranged from 201-3044 oocytes depending on fish size. Spawning shoals are segregated by sex, as indicated by commercial samples, with a biased female-to-male ratio of 4.5:1 during the spawning season (1.2:1 during the non-spawning season). In addition, features of the oocyte surface were closely examined, which revealed that the filaments on the chorion of the hydrated oocyte are adhesive. These adhesive filaments presumably allow the fertilised egg to become attached to vegetative substrate by adhesion and/or entanglement.

*H. melanochir* larvae were discriminated from another hemiramphid species, river garfish (*H. regularis*), which is also known to occur in the study area, based on species-specific amplification of part of the mitochondrial control region using a multiplex polymerase chain reaction (PCR) assay. The species were easily discerned by the number and distinct sizes of PCR products [*H. melanochir*, 443 bp; river garfish (*H. regularis*), 462 and 264 bp]. Although based on a single gene, this molecular method will correctly identify the species of individuals in at least 96% and 94% of tests for *H. melanochir* and *H. regularis*, respectively.

Subsequent to verifying the identification of species by molecular discrimination, the larval development of *H. melanochir* and *H. regularis* were described. Larvae of *H. melanochir* and *H. regularis* had completed notochord flexion at hatching and are characterized by their elongate body with distinct rows of melanophores along the dorsal, lateral and ventral surfaces; small to moderate head; heavily pigmented, long straight gut; persistent preanal finfold; and extended lower jaw. Fin formation occurs in the sequence: caudal, dorsal and anal (almost simultaneously), pectoral, pelvic. Despite the similarities between both species and among hemiramphid larvae in general, *H. melanochir* larvae are distinguishable from *H. regularis* by: having 58-61 vertebrae (v. 51-54 for *H. regularis*); having 12-15 melanophore pairs in longitudinal rows along the dorsal margin between the head and origin of the dorsal fin (v. 19-22 for *H. regularis*); and the absence of a large ventral pigment blotch anteriorly on the gut and isthmus (present in *H. regularis*). A logistic regression analysis of body measurements also revealed interspecies differences in the combined measurements of eye diameter

and pre-anal fin length. Both species can be distinguished from morphologically similar larvae found in southern Australia (other hemiramphids and a scomberosocid) by differences in meristic counts and pigmentation.

*Hyporhamphus melanochir* larvae were successfully collected throughout Gulf St Vincent using a neuston net; however, attempts to sample eggs were unsuccessful. Abundances of larvae in the gulf averaged 4.8 and 12.3 larvae 1000 m<sup>-2</sup> of surface water in December 1998 and December 2000, respectively. Larvae exhibit fast growth, as indicated by otolith growth increments, with back-calculated spawning dates falling within the October-March spawning season. Spatial analysis of larval distributions revealed a positive spatial autocorrelation, i.e. non-randomness or clustering of similar abundance values. Most larvae were found in the upper region of the gulf, and the prevalence of seagrass habitat throughout this region supports the view that the demersal eggs of *H. melanochir* become attached to seagrass and/or algae following spawning. A gyre in waters of the upper gulf, influenced by prevailing southerly winds, the Coriolis effect, and land boundaries, may explain retention of larvae. The importance of seagrass beds to *H. melanochir* spawning is also supported by anecdotal evidence and available literature on eggs of other Beloniformes, which are also demersal and attach to marine plants.

Dual stable isotope analysis ( $\delta^{13}\text{C}$  and  $\delta^{15}\text{N}$ ) of larval, juvenile and adult *H. melanochir* and several potential food sources from the Bay of Shoals was carried out to estimate the importance of zosteracean seagrass towards the assimilated diet of *H. melanochir*. Although the diet of *H. melanochir* larvae is probably planktonivorous, their isotopic signatures partly reflect the parental diet due to the influence of pre-existing tissue in addition to growth. According to mixing model calculations, the signatures of juveniles can be explained by a diet consisting of 23-37% *Zostera*, 0-10% *Halophila* and the remainder zooplankton, whilst the diet of adults consists of 53-58% *Zostera* and the remainder zooplankton. These findings indicate an increasing dependence upon *Zostera* with growth of *H. melanochir*.

The results of this study enhance the completeness of our understanding of the fisheries biology and ecology of *H. melanochir*. Significant contributions are provided in reproductive biology and larval biology, seagrass beds (in combination with mixed algae) are demonstrated to be an important habitat for spawning, and *Zostera* seagrass is shown to be a necessary food source in the diet of juveniles and adults.

## Declaration

This work contains no material which has been accepted for the award of any other degree or diploma in any university or other tertiary institution and, to the best of my knowledge and belief, contains no material previously published or written by another person, except where due reference has been made in the text.

I give consent to this copy of my thesis, when deposited in the University Library, being available for loan and photocopying.

A handwritten signature in blue ink that reads "Craig Naell". The signature is written in a cursive style with a large initial 'C'.

January 11, 2005

## Acknowledgments

This PhD study was undertaken at the University of Adelaide and was funded by an Australian Postgraduate Award (Industry) grant, with the South Australian Research & Development Institute (SARDI) – Aquatic Sciences providing in-kind support as the industry partner.

In addition to these supporting organisations, I am sincerely grateful to the following individuals:

- My supervisors Dr Mike Geddes and Dr Keith Jones for your kindness, expertise, guidance and encouragement, and for always leaving your doors open for me to discuss my work. I have great respect for you both – you’ve been excellent mentors.
- Dr Qifeng Ye for your friendship, encouragement and generosity, and always offering praise for my work. It is a great pleasure to have had the opportunity to collaborate with you during the FRDC national garfish project and to also work under your leadership in Inland Waters research at SARDI.
- David McGlennon for promoting the research of garfish in South Australia (along with my supervisors), which led to the funding for this study. Thank you for your guidance as a ‘third’ supervisor in the initial stages of my research before you went overseas.
- David Short (‘Shorty’), Wetjens Dimmlich (‘Wetch’), Dr Lianos Triantafillos (‘Big A’) and Danny Brock for being brilliant mates, and also for selflessly helping me with my fieldwork and computing problems. It has been great to share and experience similar interests with each of you both at work and away from work.
- Dr Yongshun Xiao for your friendship, generosity and advice, and making me feel like I can discuss any issue with you. I’m glad to be able to help you with using Sigmaplot – I’m not an expert, but thank you for saying that I am anyway!
- Dr Tony Fowler for providing me with my first opportunity to conduct fisheries research at SARDI, thereby allowing me to get my ‘foot in the door’ and be chosen to do this Ph.D. study. Thank you for providing excellent advice on fisheries research and scientific writing, and for improving manuscripts whenever I’ve asked for your help.
- John Ling for reviewing my reproduction chapter.
- David Taylor (from Drs King & Mower – Histopathology & Cytopathology) and Dr Marilyn Henderson (Centre for Electron Microscopy & Microstructural Analysis) for technical help with anything to do with histology or electron microscopy.
- Dr Steve Donnellan (South Australian Museum) for allowing me access to catalogued garfish specimens and teaching me a bit about genetics. I am very grateful for your expertise, generosity and encouragement, and your help with analysis of molecular data and getting our results published.
- Ralph Foster and Leanne Haigh (South Australian Museum) for giving up your time to help me develop a PCR assay and for guidance with DNA methods.
- Dr Patrick Coutin and David McKeown (Marine & Freshwater Research Institute), Gavin Wright (‘Gus’), and N.S.W. Fisheries for assisting me with obtaining garfish samples from various locations across southern Australia.

- Dr Alan Jordan (Tasmanian Aquaculture & Fisheries Institute) for donating egg and larvae specimens for my research, helping me search for distinguishing characteristics and for reviewing a manuscript.
- Barry Bruce (CSIRO Marine Research), Dr Francisco Neira ('Pancho') (Australian Maritime College) and Tom Trnski (Australian Museum) for providing tips on larval drawing techniques and reviewing a manuscript.
- Dr Suzy Ayvazian (Western Australian Marine Research Laboratories) for allowing me to conduct part of my research in your estuarine fish laboratory.
- Val Boxall, Dr Karina Hall, Bruce Jackson and Graham Hooper for either being my dive buddy or driving the boat at various times in my quest to find garfish eggs.
- The crew of RV *Ngerin* for operating the research cruises in the gulfs for the collection of larvae.
- Paul Jennings for helping me search for a suitable ageing method.
- John Vorstenbosch and Jeff Wait for assisting in the collection of samples of garfish for the reproductive biology component of my research.
- Michelle Winning (Centre for Catchment & Instream Research, Faculty of Environmental Sciences, Griffith University) for performing stable isotope analysis of garfish and dietary items.
- Prof. Bryan Womersley (State Herbarium of South Australia) and Paul Rogers for helping me identify marine plants and zooplankton.
- Mum, Dad, Scott, Jenny, Bradley and Kieran. I couldn't have done this without your love and support. You've always been there for me.
- Most of all ...Sarah. Thank you 'Beautiful.' Thank you for the love, support, encouragement and time you have given me throughout my studies – I know how much you've sacrificed for me. You've only ever known me to be studying. I'm looking forward to spending more fun times together.